Pediatr Radiol (2015) 45:1016–1025
DOI 10.1007/s00247-014-3255-y

ORIGINAL ARTICLE

Corpus callosum thickness on mid-sagittal MRI as a marker of brain volume: a pilot study in children with HIV-related brain disease and controls

Savvas Andronikou · Christelle Ackermann · Barbara Laughton · Mark Cotton · Nicollette Tomazos · Bruce Spottiswoode · Katya Mauff · John M. Pettifor

Received: 22 February 2014 / Revised: 24 July 2014 / Accepted: 25 November 2014 / Published online: 27 January 2015

Abstract
Background Corpus callosum thickness measurement on mid-sagittal MRI may be a surrogate marker of brain volume. This is important for evaluation of diseases causing brain volume gain or loss, such as HIV-related brain disease and HIV encephalopathy.

Objective To determine if thickness of the corpus callosum on mid-sagittal MRI is a surrogate marker of brain volume in children with HIV-related brain disease and in controls without HIV.

Materials and methods A retrospective MRI analysis in children (<5 years old) with HIV-related brain disease and controls used a custom-developed semi-automated tool, which divided the midline corpus callosum and measured its thickness in multiple locations. Brain volume was determined using volumetric analysis. Overall corpus callosum thickness and thickness of segments of the corpus callosum were correlated with overall and segmented (grey and white matter) brain volume.

Results Forty-four children (33 HIV-infected patients and 11 controls) were included. Significant correlations included overall corpus callosum (mean) and total brain volume (P=0.05); prefrontal corpus callosum maximum with white matter volume (P=0.02); premotor corpus callosum mean with total brain volume (P=0.04) and white matter volume (P=0.02), premotor corpus callosum maximum with white matter volume (P=0.02) and sensory corpus callosum mean with total brain volume (P=0.02).

Conclusion Corpus callosum thickness correlates with brain volume both in HIV-infected patients and controls.

Keywords Corpus callosum · Brain volume · Human immunodeficiency virus encephalopathy · Magnetic resonance imaging · Children

S. Andronikou (✉)
Department of Radiology, Faculty of Health Sciences,
University of the Witwatersrand,
South Africa, 700 Harbouredge, 10 Hospital Str. Greenpoint,
Cape Town 8005, South Africa
e-mail: docsav@mweb.co.za

C. Ackermann
Department of Radiology, University of Stellenbosch,
Stellenbosch, South Africa

B. Laughton · M. Cotton
Children's Infectious Diseases Research Unit,
Stellenbosch University and Tygerberg Children's Hospital,
Stellenbosch, South Africa

N. Tomazos
Faculty of Commerce, Department of Management Studies,
University of Cape Town, Cape Town, South Africa

B. Spottiswoode
MRC/UCT Medical Imaging Research Unit,
Department of Human Biology, University of Cape Town,
Cape Town, South Africa

K. Mauff
Department of Statistical Sciences, University of Cape Town,
Cape Town, South Africa

J. M. Pettifor
MRC/Wits Developmental Pathways for Health Research Unit,
Department of Paediatrics, Faculty of Health Sciences,
University of the Witwatersrand,
Witwatersrand, South Africa

Introduction

Human immunodeficiency virus encephalopathy is an acquired immunodeficiency syndrome (AIDS) defining event [1] occurring in vertically infected infants and children with loss of brain growth, motor abnormalities and cognitive dysfunction [2, 3]. A

sensitive predictive marker of encephalopathy is critical [4, 5] because early additional neuroprotective treatment may preserve brain integrity, slow deterioration or partially improve symptoms [3, 5, 6]. There is evidence that suggests that intensive anti-retroviral therapy may halt or even reverse encephalopathy, leading to improved neurocognitive outcome and survival in children with HIV dementia [4, 7, 8].

Ances and colleagues [5] noted that decreases in brain volume in HIV-infected adults included a decrease in volume of the corpus callosum. Chiang [9] and Dewey [10] also showed changes in corpus callosum volume in patients with HIV. Thompson et al. [11] proposed that white matter deficits might be easier to detect at the midline than globally. They suggested the use of corpus callosum thickness as an MRI marker of white matter integrity in adults with AIDS [11]. This has set the groundwork for testing this hypothesis in children. We believe that corpus callosum thickness overall and at individual segments can be used to assess white matter volume loss. Currently, because there is no available technique for measuring brain volume (or corpus callosum volume) rapidly in the clinical setting, a linear thickness of the corpus callosum may represent a rapid surrogate measure. This thickness measurement can be achieved rapidly by simply placing the measurement cursors, available on all MRI scanners at recommended locations. Our literature search did not reveal any previous studies of corpus callosum thickness as a surrogate marker of white matter volume loss in children with HIV. There are, however, previous publications using corpus callosum thickness in HIV-infected adults. Say: Thompson and colleagues [1] showed significant thinning of the corpus callosum involving predominantly the anterior three sectors (up to 25% thinner than controls) in HIV-infected adults.

Materials and methods

In a cross-sectional study, the corpus callosum was measured retrospectively on MRI in children with laboratory-confirmed vertically acquired HIV and in uninfected controls. The HIV-infected children had undergone MRI because they were diagnosed with HIV-related brain disease as part of a larger, prospective study running over 2.5 years at a referral hospital in South Africa. All patients considered for inclusion were positive for HIV DNA polymerase chain reaction, confirmed by plasma HIV RNA >1,000 copies/ml. All patients were being treated on various anti-retroviral therapy regimes at the time of imaging. The children were all African and mixed race and hailed from a low socioeconomic background.

Inclusion criteria for HIV-infected children

Clinicians had referred children on anti-retroviral therapy who had HIV-related brain disease to MRI as defined by at least one of the following findings in the absence of a concurrent illness, or environmental/ social reasons that could explain the findings:

- Locomotor developmental delay

Confirmed on Griffiths Mental Development Scales: Quotient drop of 15 (= 1 standard deviation) or a Locomotor quotient <80 that persists for at least 2 months.

Confirmed on Molteno Adapted Scale with ≥6 months' delay persisting for at least 2 months.

- Language developmental delay

Confirmed on Griffiths Mental Development Scales: Quotient drop of 15 (= 1 standard deviation) or a language quotient <80 that persists for at least 2 months, and with a normal hearing test. Confirmed on Molteno Adapted Scale with ≥6 months' delay persisting for at least 2 months.

- Brisk reflexes fulfilling one of the following criteria:

Spreads to other areas, sustained clonus, can elicit a reflex with a tap above or below tendon area.

Exclusion criteria of HIV-infected children

Children were excluded if they had any history of birth hypoxia; opportunistic or other infection of the central nervous system; systemic cytomegalovirus infection; severe illness requiring intensive care admission; gastroenteritis with hypernatremia; any near-death experience of documented event of prolonged hypoxia and/or hypotension that did not require intensive care unit (ICU) admission; prolonged hospitalization (>2 weeks) in the 3 months prior to the onset of symptoms; lack of stimulation, social neglect and possible lack of parental insight.

Patients were also excluded when MRI scans were unavailable, incomplete or inadequate.

Inclusion criteria of HIV-uninfected controls

These were obtained using clinically indicated MRI scans of HIV-negative children matched for age and gender, referred for headache and reported as being normal. A pediatric neuroradiologist reviewed the MRI scans to confirm that there were no pathological findings on imaging (i.e. two evaluations of the imaging confirming a normal brain MRI). Children with abnormal neurological clinical assessments were excluded from the control group through review of the charts.

HIV-infected patients and controls were also excluded later in the study whenever volumetric analysis (described below) did not result in adequate images for assessment.

MRI scanning was performed on a Magnetom Symphony 1.5 T (Siemens, Erlangen, Germany). Axial T2-W: TE 103, TR 5,460, slice 5 mm and gap 1.5 mm. Sagittal T1-W: TE 14, TR 531, slice 5 mm, gap 1.5 mm when available; matrix: 512 × 512.

Measurement instruments and data

Overall mean and maximum corpus callosum thickness in millimeters (mm) were calculated using software developed in-house (by B.S.) by importing MRI data into a customized tool written in MATLAB (The Mathworks Inc., Natick, MA). MATLAB is a high-level language and interactive environment that enables you to perform computationally intensive tasks faster than with traditional programming languages such as C, C++ and Fortran. A description of this method was published in 2012 [12] and is similar to the method of Luders and colleagues [13] but creates up to 40 thickness measures rather than 100. The operator (S.A.) selected the midline sagittal T1-weighted image for each patient and then dorsal (top) and ventral (bottom) corpus callosum contours were manually drawn using a point depositing system. This initiated automated calculation of a contour midway between the contours (referred to in other publications as the corpus callosum diameter) [14]. The program then divided the midline contour into segments with perpendicular spokes projected from each segment until they intersected with the dorsal and ventral contours (Fig. 1). The number of segments was limited by the spatial resolution of diffusion tensor imaging because the software was also intended for generating fiber tracts from corpus callosum seeds (part of future research). A maximum of 40 segments was chosen for this application to ensure that each segment still consisted of a contiguous strip of voxels across the corpus callosum. The system automatically plotted segment thickness as a function of distance along the midline corpus callosum contour (Fig. 1). *Mean and maximum thickness* were determined for each segment as previously described [15–17] by including thickness of all measurements within each segment. The segments were defined as: prefrontal (anterior sixth); pre-motor (between anterior sixth and the midpoint); motor (midpoint to posterior third); sensory (posterior third to posterior quarter) and language/visual (posterior quarter) (Fig. 2).

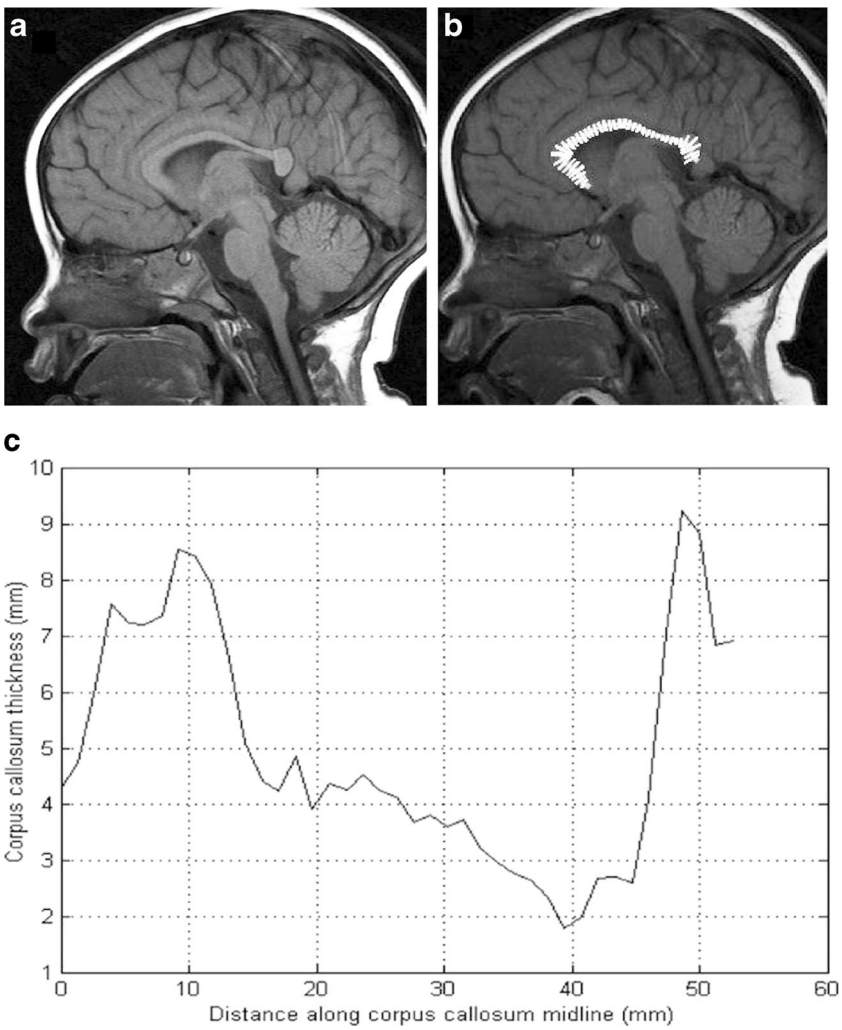

Fig. 1 Corpus callosum thickness measurements with graphic representation in a 2-year-old girl. Midline sagittal T1-W MRI (**a**) and midline sagittal T1-W MRI (**b**) of the corpus callosum indicating the 40 radial measurements of thickness produced by the custom semi-automated tool. Thickness measurments (**c**) are automatically plotted vs. length (diameter) of the corpus callosum

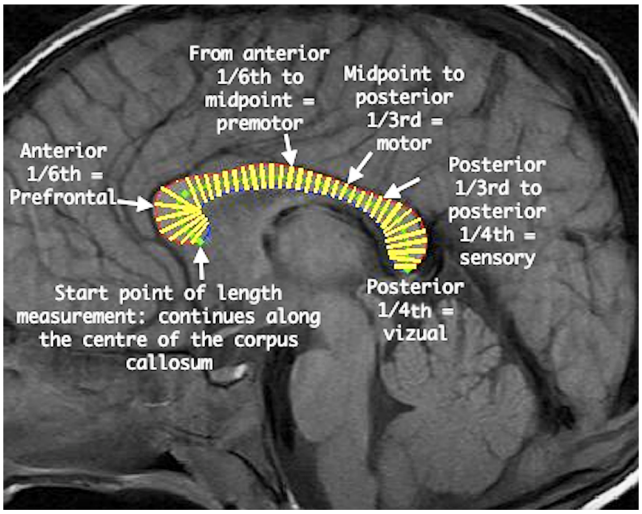

Fig. 2 Predefined anatomical segments of the corpus callosum are demonstrated on a sagittal midline T1-weighted image based on the number of radial thickness measurement markers in a 2-year-old boy. All thickness measurements within each section were used to determine mean and maximum segmental thicknesses. The length was measured automatically along the central arc as indicated by the start point

Corpus callosum length (from tip of rostrum midpoint to tip of splenium midpoint) was derived automatically.

Brain volume calculation: Total brain volume, grey matter volume and white matter volume were calculated from axial T2-W in each patient using MATLAB 7.3 (The Mathworks Inc., Natick, MA) and Statistical Parametric Mapping software (SPM5; Wellcome Department of Imaging Neurosciences, University College, London) using voxel-based morphometric analysis. Use of the T2-weighted sequence for SPM segmentation and volume calculation has precedent in the work by Carone et al. [18] and von Bezing et al. [19]. This is a whole-brain technique for characterizing volume and tissue "concentration" differences in structural MRIs. The MRI scans were spatially normalized toward a template of normal paediatric MRI scans released by the Imaging Research Center, Cincinnati Children's Hospital Medical Center. The normalized images were then segmented into grey matter and white matter and volumes in milliliters of each were derived using the automated volume calculation Easy Volume (Fig. 3). Total brain volume was determined by summing the calculated grey matter and white matter volumes. The primary investigator (S.A.), who has more than 14 years of pediatric neuroimaging experience, performed neuroimaging analysis. To determine reliability of the thickness measurement, a second operator (B.S.), a biomedical engineer, performed separate blinded measurement of thickness of the corpus callosum using the custom software tool.

Data analysis

Data were summarized using mean and standard deviations for continuous normally distributed variables and median and range when data were not normally distributed (age, corpus callosum thickness [mm],corpus callosum length [mm], total brain volume, grey matter volume, white matter volume [ml]). Categorical variables (patients/controls; males/females) were recorded as frequencies and percentages. Pearson correlations were used for normally distributed values and Spearman correlations for non-normally distributed values. Overall mean and maximum thickness of the corpus callosum as well as segmental mean and maximum thickness were correlated against brain volume (total brain volume, grey matter and white matter volumes) for both patients and controls. Comparisons between patients and controls were performed using independent *t*-tests or Mann–Whitney tests (for continuous non-normally distributed variables) with regard to overall mean corpus callosum thickness, mean segmental thicknesses and white matter volume. Significance was considered if $P<0.05$.

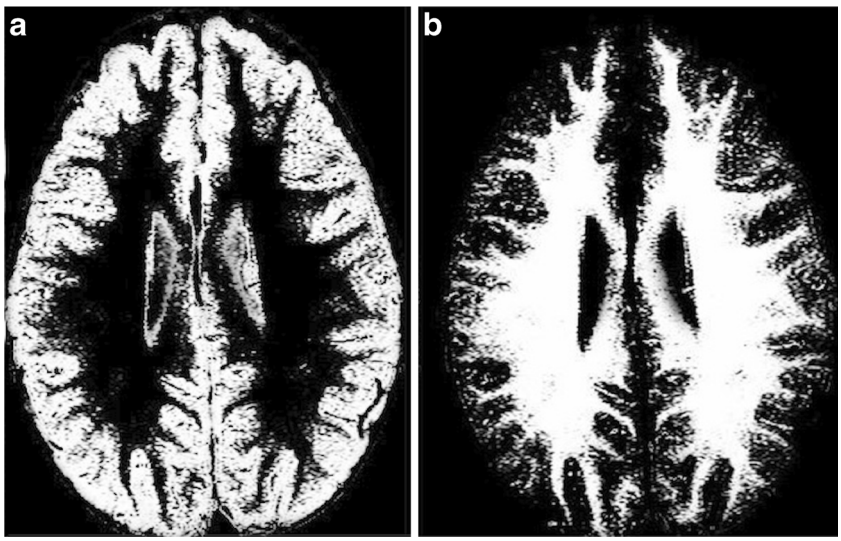

Fig. 3 Representative axial images with segmented white and grey matter for volume calculation in a 2-year-old girl (same patient as Fig. 1). Image produced using segmentation techniques (**a**) indicates the segmented grey matter from which volume was derived. Image produced using segmentation techniques (**b**) indicates the segmented white matter from which volume was derived

Table 1 Overall and segmental mean corpus callosum (CC) thickness (mm) for controls and patients

	Controls			Patients		
Variable	*n*	Mean±SD or Median (IQR)	Min–Max	*n*	Mean±SD or Median (IQR)	Min-Max
Overall CC	11	5.74±1.02	3.7–7.6	33	5.54±0.64	3.9–6.9
Prefrontal CC	11	7.44±1.45	5.2–10.4	33	7.34±1.09	4.8–10.5
Premotor CC	11	5.50±1.16	3.4–7.4	33	5.53±0.66	4.4–7.3
Motor CC	11	4 (3.8–4.8)	2.7–6.2	33	4.1 (3.6–4.3)	2.6–6.5
Sensory CC	11	3.5 (3–4.5)	2.3–5.3	33	3.2 (2.6–4)	2.2–5.1
Visual CC	11	6.73±1.17	3.7–8.3	33	6.22±1.17	3.5–8.5

IQR inter-quartile range, *SD* standard deviation

Interobserver agreement between the two independent operators' determination of a mean of each corpus callosum segment and the overall mean thickness of the corpus callosum was tested using a two-way agreement model to determine the intraclass correlation coefficient (ICC) and a standard error of measurement (SEM).

Ethics

MRI studies were performed for clinical indications. Two institutional ethics review boards approved the study (N07/09/208) (M110802).

Results

A total of 56 children had MRI scans for HIV-related brain disease and were considered for inclusion. Only 48 met the inclusion criteria. Sixteen controls were selected to meet the control inclusion criteria. Exclusion criteria resulted in 4 patients being excluded because imaging was lost, and an additional 11 patients and 5 controls being excluded because of motion artifacts after the volumetric analysis. This resulted in a study population of 44 with 33 HIV-infected patients and 11 uninfected controls. HIV-infected patients' age ranged from 7 to 49 months (median: 31 months; mean: 30 months) and there were 16 boys and 17 girls. Controls ranged in age from 13 to 48 months (median: 34 months; mean: 32 months) and there were 6 boys and 5 girls.

Corpus callosum thicknesses of patients and controls are summarized in Tables 1 (mean) and 2 (maximum). Brain volumes are summarized for patients and controls in Table 3. There were no significant differences between HIV-infected patients and uninfected controls.

Significant correlations included: Overall corpus callosum (mean) with total brain volume (P=0.05; correlation coefficient 0.2992); prefrontal corpus callosum maximum with white matter volume (P=0.02; correlation coefficient 0.3528); premotor corpus callosum mean with total brain volume (P=0.04; correlation coefficient 0.3126) and white matter volume (P=0.02; correlation coefficient 0.3536), premotor corpus callosum maximum with white matter volume (P=0.02; correlation coefficient 0.3429) and sensory corpus callosum mean with total brain volume (P=0.02; correlation coefficient 0.3457). The only significant correlation with age was the premotor corpus callosum mean thickness in (P=0.04; correlation coefficient 0.3089).

Interobserver agreements were: length measurement, ICC=0.31, SEM=2.47; overall corpus callosum thickness, ICC=0.80, SEM=0.348; prefrontal section measurement, ICC=0.86, SEM=0.44; premotor corpus callosum, ICC=0.77, SEM=0.33; motor corpus callosum, ICC=0.74, SEM=0.39; sensory corpus callosum, ICC=0.59, SEM=0.58; visual corpus callosum, ICC=0.67, SEM=0.83.

Table 2 Overall and segmental maximum corpus callosum (CC) thickness (mm) and length (mm) for controls and patients

	Controls			Patients		
Variable	*n*	Mean±SD or Median (interquartile range)	Min-Max	*n*	Mean±SD or Median (interquartile range)	Min - Max
CC length	11	46.7±2.8	41.1–50.7	33	48.9±2.7	41.3–54.7
Overall CC	11	9.4±1.6	6.3–11.6	33	9.3±1.2	6.6–11.6
Prefrontal CC	11	9±1.7	6.3–11.6	33	8.7±1.4	6.3–11.5
Premotor CC	11	7.6±1.7	4.8–10	33	7.5±1	5.9–10.4
Motor CC	11	4.6 (4.4–5.2)	3.3–6.8	33	4.6 (4.4–5.1)	3.5–6.9
Sensory CC	11	4.1±1	2.7–6	33	3.7±0.9	2.4–5.4
Visual CC	11	8.6±1.6	4.6–10.5	33	8.4±1.4	4.6–11.6

SD standard deviation

Table 3 Brain volumes (ml) for controls and patients

	Controls			Patients		
Variable	*n*	Mean±SD	Min-Max	*n*	Mean±SD	Min-Max
Grey matter	11	647.36±107.00	500–857	33	631.94±75.67	500–800
White matter	11	326.91±51.62	269–423	33	354.85±45.12	257–430
Whole brain	11	974.27±147.95	774–1,280	33	986.79±93.29	820–1184

SD standard deviation

Discussion

The corpus callosum size changes through childhood [14, 17, 20–22] with the anterior corpus callosum (rostrum and genu) reaching maximum size earlier [17] (gaining adult thickness at 5–6 years-of-age) [22]. Garel et al. [14] published corpus callosum thickness reference values and reported no difference between boys and girls. We preferred local controls rather than using the normative data in our study because we had a different African population from impoverished backgrounds that may have been affected by malnutrition and other environmental factors.

Wilde et al. [23] report that the anterior portions of the corpus callosum change the least with age and can be used for reference referring to patients older than 1 year of age. Mean/median age of both patients and controls in our study was greater than 2 1/2 years. Prefrontal corpus callosum thickness in our patients and controls correlated the least with age (P=0.98), supporting the anterior region's thickness stability over age groups. The only part of the corpus callosum that correlated with age (in patients only) was the premotor segment (P=0.0413), which is central. The most recent morphological data, obtained by Garel and colleagues [14] from 622 children using MRI, demonstrate that there is rapid growth until 3 years of age, after which stabilisation of the isthmus-splenial thickness ratio occurs (considered indicative of corpus callosum modelling). Our interpretation of this study's findings would support the use of the anterior prefrontal segment as a marker of normality due to its early development and stability over age.

Thickness of the corpus callosum is affected by peripheral white matter loss, making it a surrogate for white matter atrophy [11]. Hasan et al. [17] proposed using corpus callosum volume as a surrogate marker of brain volume. We investigated the correlation of segmental corpus callosum thickness rather than corpus callosum volume with brain volume because radiologists are more likely to use thickness, through simple caliper measurements, in clinical practice. We recommend using the prefrontal measurement, which we showed to correlate with white matter volume (P=0.0188), because it is easily identified as the most anterior portion (the genu) and because of its stability over age groups (mentioned above). A median prefrontal corpus callosum segment thickness measurement (based on our controls) of 9 mm (interquartile range: 7.4–10.3 mm) should be considered when evaluating African patients. For normal European 3-year-old children, the thickness value expected at the genu is very similar at 9.1 mm (3rd–97th percentile: 6.3–11.8 mm) [14]. HIV leukoencephalopathy includes diffuse myelin loss, astroglial proliferation, and infiltration by mono and multinucleated macrophages [24]. Children younger than 2 years of age have described patterns of central nervous system involvement in HIV infection, which differ from those in adults [25].

Neuroimaging has been utilized to follow the course of those HIV-infected children with neuropsychological problems [26] with three clear roles: (a) it is a screening tool for detection of cerebral atrophy; (b) it is a diagnostic tool for detection of complications such as lymphoma, stroke and opportunistic infections, and (c) it is useful for follow-up after initiation of anti-retroviral therapy to determine response to treatment [27]. MRI screening for atrophy has therefore been suggested for children at high risk for encephalopathy and is advisable when evidence of neurological symptoms or neurocognitive dysfunction is noted [28].

The most common imaging findings in children with HIV encephalopathy are basal ganglia calcification and atrophy [1, 29, 30]. In one study (from 1998), every child with a diagnosis of encephalopathy had a positive neuroimaging finding – either atrophy or basal ganglia calcification [30]. Cerebral atrophy and ventriculomegaly were present in 68% and 78%, respectively, of HIV-infected children with symptomatic disease [1].

Interpretation of standard structural MRI lacks the sensitivity to detect subtle volume loss and white matter abnormalities in HIV-related brain disease [9]. Volumetric techniques are therefore valuable for identifying subtler structural changes in the brain [10]. Ances and colleagues [5] have suggested that brain volume assessment may be a more robust way of quantifying brain integrity in adults with HIV. Manual delineation of the brain by trained experts is the gold standard for determining the volume of structures, but automated techniques are preferred because manual measurements are extremely labour-intensive and time-consuming [9, 11]. Most clinical researchers use Statistical Parametric Mapping (SPM, Wellcome Trust Centre for Neuroimaging, UK), which is automated and therefore less labour-intensive but not automated enough for clinical use [9, 11]. This drives the ongoing search for clinically useful and quick surrogate methods reflecting brain volume and clinical parameters [11].

The aim of management is to rapidly identify HIV-infected infants at risk of central nervous system disease progression and to institute effective treatment that can halt devastating

effects of HIV on the developing brain [2]. MRI may have a role to play in this early detection of HIV encephalopathy and in the prediction of developmental outcome without and with treatment [24]. HIV-infected patients are expected to demonstrate cerebral atrophy [1, 29, 30]. Our HIV-infected patients did not differ significantly from controls in corpus callosum thickness or volume. Figure 4 is an example of an 18-month-old boy with HIV-related brain disease who underwent corpus callosum thickness/length measurements and brain volume determination but did not show significant thinning of the corpus callosum compared to age-matched controls. Possible reasons for this, in the order of most likely to least likely, include:

(a) The definition of HIV-related brain disease in our study does not equate to HIV encephalopathy, i.e. even though white matter pathology may be present, atrophy/ volume loss may not be established yet. Mean Griffiths Mental Development Scales in our HIV-infected patients fell into a low average category, which is approximately only one standard deviation lower than HIV-uninfected children reported in the literature [31]. Significant developmental delay is regarded as<two standard deviations below mean (i.e. <70). This milder brain disease in our patients may account for the lack of atrophy/ brain volume loss in our study.

(b) HIV encephalitis may occur while patients are on anti-retroviral therapy [11] and possibly reflects Immune Reconstitution Inflammatory Syndrome, which affects up to 37% of patients starting treatment [32] and may therefore manifest with volume gain of the brain. All our patients were on anti-retroviral therapy for a mean of +/− 100 days at the time of imaging.

(c) Controls may have had low brain volumes due to malnutrition [33] or other chronic infections. Our controls were not normal, but rather, comprised children with normal MRI scans, keeping in mind that subjective MRI reporting as well as the review by the pediatric neuroradiologist lacks sensitivity for subtle volume loss [34]. This logic suggests that brain volume and consequently corpus callosum volume and thickness should be considered in tandem with nutritional assessment, which was not assessed in this research. The controls were not known to have other chronic infections.

Since 2007, seven studies of corpus callosum thickness have included children and adolescents [21, 22, 35–39]. Factors correlated with corpus callosum thinning have included hydrocephalus, mental retardation, sickle cell disease, spastic quadraparesis, neoplasia, preterm birth [37], periventricular leukomalacia, white matter atrophy, motor performance, IQ [38, 39], attention deficit hyperactivity disorder [35] and foetal alcohol syndrome [21]. None has specifically correlated corpus callosum thickness with brain volume in HIV. The proposed use of this simple clinical measurement on standard sagittal MRI in detecting brain atrophy in children infected

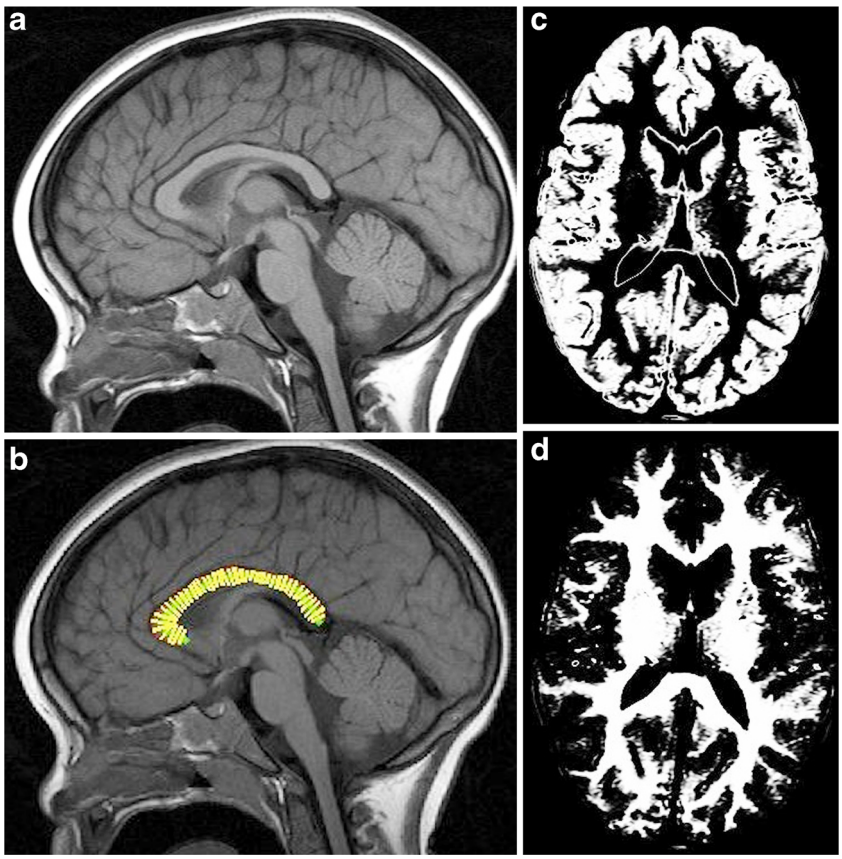

Fig. 4 An 18-month-old boy with HIV-related brain disease and failure of brain growth underwent corpus callosum thickness/length measurements and brain volume determination. Midline sagittal T1-W MRI of the corpus callosum (**a**). Midline sagittal T1-W MRI of the corpus callosum (**b**) indicates the radial measurements of thickness produced by the custom semi-automated tool. Grey matter segmentation for volume assessment (**c**). White matter segmentation for volume assessment (**d**)

with HIV has significant clinical significance for children who stand to benefit from targeted treatment.

Limitations

There are several limitations related to the study. Firstly, patient and control subject numbers are relatively small. Fifteen patients and five controls were lost or excluded due to the inability to adequately assess brain volume calculations as recommended in previous publications [10]. This makes the volumetric analysis more accurate, however. Secondly, the control subjects we used could not be classified as totally normal as all had clinical reasons for MRI. The need for anaesthesia/sedation for MRI in children younger than 6 years of age precluded the use of normal children as controls. The main objective of our study, however, was to correlate corpus callosum thickness with volume and not to develop normative values.

On the technical side, semi-automated corpus callosum thickness measurements have limitations:

(a) Selection of the midline is influenced by the thickness and number of sagittal slices. The thinner the slices, the more options there are for selecting the midline slice, which would affect repeatability. Our thicker standard sagittal MRI slices limited this selection and represents standard practice.

(b) Point deposition on the corpus callosum was operator-dependent both with regard to the number of points deposited and the site where these were deposited. There were no prescribed landmarks for depositing points. This will be true in the clinical setting also. The following comments are also worth noting; the inferior corpus callosum margin and rostral edge were frequently indistinct; the union of the fornix with the corpus callosum obscures the inferior margin; start/end points are not defined anatomical points and the physical thickness of the marker dot can affect placement. The semi-automated tool was easy to use, however, and contrast resolution in MRI is superior to all other medical imaging modalities.

(c) Operator agreement: ICC is interpreted similar to correlation. It's always difficult to say what is good and what is poor agreement because it is all relative. So relative to each other, the above is probably correct. The SEM can be seen as a measure of the expected difference between the raters expressed in the same units as the measurements. We therefore interpret our results a good agreement on overall corpus callosum thickness and prefrontal thickness, moderate agreement on premotor, motor and visual thickness and poor agreement on overall length measurement.

The customized tool used in our study differs to one used by Luders [22] by providing a maximum of 40 segments rather than 100. It was designed for use with diffusion tensor imaging where segments serve as seeds for fiber tracking and ensures that segments consist of a contiguous strip of voxels [12]. It should be noted, however, that this tool was only validated with regard to its functionality and was initially used in only seven subjects. No diffusion tensor imaging was used for this study and the software is intended for use in diffusion tensor imaging in ongoing research. A number of recent papers describe methods for semi-automated and fully automated measurement of corpus callosum thickness on MRI. Most notable are those by Adamson in 2011 [40] and Herron in 2012 [41]. Herron describes a variety of techniques that are either semi-automated, which like our method require manual outlining of the corpus callosum , or fully automated including the boundary-based and rule-based approaches. These authors acknowledge that measurement of the corpus callosum thickness on MRI is complicated by variability of size, shape and location and that manual outlining may be required to achieve adequate performance [41]. This is important for pediatric work where there is marked variability in both size and shape over age groups due to myelination, pruning and general growth. Even the method described by Herron et al. [41] has limitations for use in children because this rule-based technique is affected by variability in white matter intensity and myelination differences. The use of a median anchor point rather than a boundary anchor point for generating thickness measures in the study by Herron et al. [41] strongly supports our technique for more accurate thickness measurement.

Conclusion

We have demonstrated that overall and segmental mid-sagittal MRI thickness of the corpus callosum correlates with brain volume in HIV-infected children and non-infected controls. We recommend using the prefrontal corpus callosum thickness (the genu), which is easy to identify and measure and correlates significantly with white matter volume, for clinical use. Even though not demonstrated in our patients, we expect that once encephalopathy is established and brain atrophy is present, corpus callosum thickness at the prefrontal and premotor area may reflect the degree of atrophy in HIV or other diseases. This will be a clinically useful tool for diagnosis of HIV encephalopathy and for following response to treatment.

Our ongoing research includes diffusion tensor imaging fractional anisotropy and fiber number determination, and correlation of corpus callosum thickness with volume in patients with true atrophy. Correlation with clinical and laboratory measurements of immunity in HIV-infected children is already underway.

Acknowledgments Support was provided by National Research Foundation of South Africa, the Medical Research Council of South Africa, the Harry Crossley Foundation, and NIH grant U19A153217 through the Comprehensive International Program of Research on AIDS (CIPRA) network. We also thank Anita Janse van Rensburg (Children's Infectious

Diseases Clinical Research Unit) for meticulous data collection and verification.

Conflicts of interest None

References

1. Gavin P, Yogev R (1999) Central nervous system abnormalities in pediatric human immunodeficiency virus infection. Pediatr Neurosurg 31:115–123
2. Fowler MG (1994) Pediatric HIV infection: neurologic and neuropsychologic findings. Acta Paediatr Suppl 400:59–62
3. Mitchell W (2001) Neurological and developmental effects of HIV and AIDS in children and adolescents. Ment Retard Dev Disabil Res Rev 7:211–216
4. Sanchez-Ramon S, Resino S, Bellon Cano JM et al (2003) Neuroprotective effects of early antiretrovirals in vertical HIV infection. Pediatr Neurol 29:218–221
5. Ances BM, Ortega M, Vaida F et al (2012) Independent effects of HIV, aging, and HAART on brain volumetric measures. J Acquir Immune Defic Syndr 59:469–477
6. Schmitt B, Seeger J, Kreuz W et al (1991) Central nervous system involvement of children with HIV infection. Dev Med Child Neurol 33:535–540
7. Czornyj LA (2006) Encephalopathy in children infected by vertically transmitted human immunodeficiency virus. Rev Neurol 42:743–753
8. Shanbhag MC, Rutstein RM, Zaoutis T et al (2005) Neurocognitive functioning in pediatric human immunodeficiency virus infection: effects of combined therapy. Arch Pediatr Adolesc Med 159:651–656
9. Chiang MC, Dutton RA, Hayashi KM et al (2007) 3D pattern of brain atrophy in HIV/AIDS visualized using tensor-based morphometry. Neuroimage 34:44–60
10. Dewey J, Hana G, Russell T et al (2010) Reliability and validity of MRI-based automated volumetry software relative to auto-assisted manual measurement of subcortical structures in HIV-infected patients from a multisite study. Neuroimage 51:1334–1344
11. Thompson PM, Dutton RA, Hayashi KM et al (2006) 3D mapping of ventricular and corpus callosum abnormalities in HIV/AIDS. Neuroimage 31:12–23
12. Andronikou S, Spottiswoode BS, Tomazos N (2012) A semi-automated method for measuring thickness and white matter integrity of the corpus callosum. SAfr J Rad 16:130–133
13. Luders E, Narr KL, Bilder RM et al (2007) Positive correlations between corpus callosum thickness and intelligence. Neuroimage 37:1457–1464
14. Garel C, Cont I, Alberti C et al (2011) Biometry of the corpus callosum in children: MR imaging reference data. AJNR Am J Neuroradiol 32:1436–1443
15. Hofer S, Frahm J (2006) Topography of the human corpus callosum revisited–comprehensive fiber tractography using diffusion tensor magnetic resonance imaging. Neuroimage 32: 989–994
16. Dougherty RF, Ben-Shachar M, Deutsch G et al (2005) Occipital-callosal pathways in children: Validation and atlas development. Ann N Y Acad Sci 1064:98–112
17. Hasan KM, Kamali A, Iftikhar A et al (2009) Diffusion tensor tractography quantification of the human corpus callosum fiber pathways across the lifespan. Brain Res 1249:91–100
18. Carone DA, Benedict RH, Dwyer MG et al (2006) Semi-automatic brain region extraction (SABRE) reveals superior cortical and deep gray matter atrophy in MS. Neuroimage 29:505–514
19. von Bezing H, Andronikou S, van Toorn R et al (2012) Are linear measurements and computerized volumetric ratios determined from axial MRI useful for diagnosing hydrocephalus in children with tuberculous meningitis? Childs Nerv Syst 28:79–85
20. Giedd JN, Rumsey JM, Castellanos FX et al (1996) A quantitative MRI study of the corpus callosum in children and adolescents. Brain Res Dev Brain Res 91:274–280
21. Yang Y, Phillips OR, Kan E et al (2012) Callosal thickness reductions relate to facial dysmorphology in fetal alcohol spectrum disorders. Alcohol Clin Exp Res 36:798–806
22. Luders E, Thompson PM, Toga AW (2010) The development of the corpus callosum in the healthy human brain. J Neurosci 30:10985–10990
23. Wilde EA, Chu Z, Bigler ED et al (2006) Diffusion tensor imaging in the corpus callosum in children after moderate to severe traumatic brain injury. J Neurotrauma 23:1412–1426
24. Thurnher MM, Schindler EG, Thurnher SA et al (2000) Highly active antiretroviral therapy for patients with AIDS dementia complex: effect on MR imaging findings and clinical course. AJNR Am J Neuroradiol 21:670–678
25. States LJ, Zimmerman RA, Rutstein RM (1997) Imaging of pediatric central nervous system HIV infection. Neuroimaging Clin N Am 7: 321–339
26. Kollar K, Jelenik Z, Hegelsberger E (2003) Neurologic aspects of HIV infections–follow-up of pediatric patients. Ideggyogy Sz 56: 397–404
27. Tucker KA, Robertson KR, Lin W et al (2004) Neuroimaging in human immunodeficiency virus infection. J Neuroimmunol 157: 153–162
28. Patsalides AD, Wood LV, Atac GK et al (2002) Cerebrovascular disease in HIV-infected pediatric patients: neuroimaging findings. AJR Am J Roentgenol 179:999–1003
29. Spreer J, Enenkel-Stoodt S, Funk M et al (1994) Neuroradiological findings in perinatally HIV-infected children. Röfo 161:106–112
30. Johann-Liang R, Lin K, Cervia J et al (1998) Neuroimaging findings in children perinatally infected with the human immunodeficiency virus. Pediatr Infect Dis J 17:753–754
31. Laughton B, Springer P, Grove D et al (2010) Longitudinal developmental profile of children from low socio-economic circumstances in Cape Town, using the 1996 Griffiths Mental Development Scales. SAJCH 4:106–111
32. Oelschlaeger C, Dziewas R, Reichelt D et al (2010) Severe leukoencephalopathy with fulminant cerebral edema reflecting immune reconstitution inflammatory syndrome during HIV infection: a case report. J Med Case Rep 4:214
33. Atalabi OM, Lagunju IA, Tongo OO et al (2010) Cranial magnetic resonance imaging findings in kwashiorkor. Int J Neurosci 120:23–27
34. Cohen RA, Harezlak J, Schifitto G et al (2010) Effects of nadir CD4 count and duration of human immunodeficiency virus infection on brain volumes in the highly active antiretroviral therapy era. J Neurovirol 16:25–32
35. Luders E, Narr KL, Hamilton LS et al (2009) Decreased callosal thickness in attention-deficit/hyperactivity disorder. Biol Psychiatry 65:84–88
36. Westerhausen R, Luders E, Specht K et al (2011) Structural and functional reorganization of the corpus callosum between the age of 6 and 8 years. Cereb Cortex 21:1012–1017
37. Luders E, Thompson PM, Narr KL et al (2011) The link between callosal thickness and intelligence in healthy children and adolescents. Neuroimage 54:1823–1830

38. Northam GB, Liegeois F, Chong WK et al (2011) Total brain white matter is a major determinant of IQ in adolescents born preterm. Ann Neurol 69:702–711
39. Narberhaus A, Segarra D, Caldu X et al (2007) Gestational age at preterm birth in relation to corpus callosum and general cognitive outcome in adolescents. J Child Neurol 22:761–765
40. Adamson CL, Wood AG, Chen J et al (2011) Thickness profile generation for the corpus callosum using Laplace's equation. Hum Brain Mapp 32:2131–2140
41. Herron TJ, Kang X, Woods DL (2012) Automated measurement of the human corpus callosum using MRI. Front Neuroinform 6:25